

## Automated ROI-Based Compression on Brain Images Using Principal Component Analysis

<sup>1</sup>Sin Ting Lim and <sup>2</sup>Nurulfajar Bin Abdul Manap

<sup>1</sup>Faculty of Engineering and Technology, Multimedia University, Melaka, Malaysia

<sup>2</sup>Faculty of Electronics and Computer Engineering, Universiti Teknikal Malaysia Melaka, Melaka, Malaysia

---

**Abstract:** Medical image contains diagnostically important regions that shall not be subjected to lossy compression. In order to increase compression rate for higher transmission and storage capability, a partial compression scheme based on ROI and non-ROI was employed. A manual segmentation technique to separate ROI and non-ROI for thousands of images are impractical, hence in this study an automated brain segmentation technique was developed to work with a PCA compression scheme. Non-ROI region will be compressed by PCA compression while ROI region will be preserved. The segmentation technique specifically tailored for brain segmentation has successfully separate ROI and non-ROI regions and results indicate that image quality is higher for image undergo the proposed model compared with image without ROI segmentation.

---

**Key words:** Medical image compression, ROI, automated segmentation, compression, important, PCA

---

### INTRODUCTION

Medical image acquired from the imaging modality such as MRI or CT scanner provides accurate anatomical or functional projections of the human body. Hence, the images need to be of adequate quality for any manual diagnosis or computerized decision support system to be reliable. In clinical practice, a medical image is produced in a standardized DICOM (Digital Imaging and Communication in Medicine) format that supports up to 2 bytes of gray level. Take an MRI image with a typical matrix format of 512×512, the total memory required to store the single MRI image is therefore, approximately 0.5 MB.

According to the national statistics by England (2016) there were about 2.9 million MRI test taken between June 2014-May 2015 and this simply sums up the total memory storage of MRI images to as large as tera bytes in annual basis. The voluminous amount of image size for all radiology modalities combined nevertheless poses a challenge to digital image storage and transmission. Hence, identifying an optimum way to compress medical images is hence, important. The methods of image compression are generally divided into two categories: lossless and lossy. Images compressed by lossless algorithm are perfectly reconstructed but the compression

ratio achieved is low. Some typical examples of lossless compression include dictionary-based LZW that is incorporated in GIF format, Run-Length Encoded (RLE) and JPEG Lossless compression Standard (JPEG-LS). On the contrary, the compression ratio for image compressed by lossy algorithm can be ten times higher than the image compressed by lossless algorithm while maintaining good visual quality. According to Canadian Association of Radiology (CAR) (Radiologist, 2011), reviews reported that lossy compression is in fact a clinically acceptable option for the compression of medical images in current practice if used and implemented appropriately. However, the discarded data of the image is non-recoverable upon decompression. Wavelet-based JPEG 2000 provides both lossless and Sin Ting Lim lossy algorithm and it is one of the algorithms recommended by the DICOM standard, together with JPEG and JPEG-LS. Besides JPEG2000, the non-standard lossy algorithms are mostly transform-based methods for examples the Principal Component Analysis (PCA) and the Discrete Cosine Transform (DCT).

The compression algorithms all serve a common purpose which is to enable the image to be represented in a more compact form while preserving maximum signal energy. Due to its optimality of signal decorrelation and energy compaction (Wang, 2012), PCA is a linear

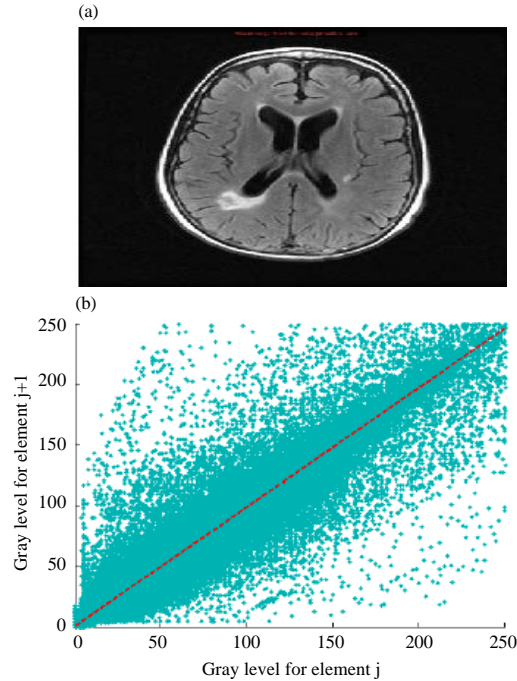


Fig. 1: a)MRI brain image and b) Scatter plot of neighboring pixel value pairs for image in (a) where the line of best fit is represented in dashed line

transformation method that can be used to remove data redundancy while retaining maximum information in data compression.

In medical images, pixel values that comes under the same anatomy features are often fall within the same scale. Therefore, medical images particularly exhibit strong correlation between its neighboring pixels. This relationships can be illustrated using a scatter plot where the gray level value for each element  $j$  of an were plotted against its adjacent pixel value  $j+1$  in x and y-axis, respectively. Scatter plot in Fig. 1b demonstrates a strong positive correlation between its neighboring pixels for the image in Fig. 1a indicating high redundancy data measurements. Since, the pixel values are predictable from the neighboring pixels, it is logical to reduce the number of variables or image dimensions by finding the line of best fit.

The line of best fit for the data points predict the value of dependent variables given the values of independent variables. While the line of best fit is the line in which the sum of square error of the vertical distance from the points to the line is minimum, principal component line of best fit is the sum of square error of the perpendicular distance from the points to the line is minimum.

PCA, introduced predominantly by Pearson (1901) and Hotelling (1933) was developed further by Dony (2001). Hence, PCA is also termed as KLT or hotelling transform. These methods differ in the way of how principal components are being derived. In this study, PCA will be explained using the theorem of linear algebra following the trend proposed by Karhunen and Loeve. Let  $X$  be a real-valued discrete random variable with density function  $f(x)$ , the variance  $\sigma^2$  is defined by:

$$\sigma^2 = E[(x-\mu)^2] \quad (1)$$

where,  $\mu$  is the mean input. If the dataset is the gray level values for an image,  $X$  will be a  $m \times n$  matrix where  $m$  denoted as the row and  $n$  the number of dimensions:

$$X = \begin{bmatrix} f(0, 0) & f(0, 1) & \cdots & f(0, n-1) \\ f(1, 0) & f(1, 1) & \cdots & f(1, n-1) \\ \vdots & \vdots & \ddots & \vdots \\ f(m-1, 0) & f(m-1, 1) & \vdots & f(m-1, n-1) \end{bmatrix} \quad (2)$$

The objective of PCA, here is to de-correlate the input data and it could be achieved by changing the basis of the input  $X$  into another output matrix  $Y$  such that the variables in  $Y$  obtain a covariance of zero and maximum signal of variance. As shown in Eq. 3, the covariance matrix of  $Y$  is a diagonal matrix:

$$\text{cov}(Y) = \begin{bmatrix} \sigma_{11} & 0 & 0 & 0 \\ 0 & \sigma_{21} & 0 & 0 \\ 0 & 0 & \ddots & \\ 0 & 0 & 0 & \sigma_{nn} \end{bmatrix} \quad (3)$$

$$Y = AX \quad (4)$$

The challenge of PCA is to find a matrix  $A$  that can linearly transform  $X$  into  $Y$  such that covariance matrix of  $Y$  meets the standards in Eq. 3. At this point of discussion, the mean of  $X$  and  $Y$  is assumed zero for convenience such that  $\text{cov}(X) = E[XX^T]$  (Schlens, 2014). The first step started with redefining covariance matrix of  $Y$  in algebraic expression:

$$\text{cov}(Y) = E[YY^T] \quad (5)$$

Substituting and rearranging the matrix notation, it arrives as:

$$\text{cov}(Y) = E[A(\text{cov}(X)A^T)] \quad (6)$$

According to theorem of linear algebra, if a matrix is symmetric it is orthogonally diagonalizable. Hence, the mathematical representation for  $\text{cov}(X)$  can be written as follow:

$$\text{cov}(X) = PDP^T \quad (7)$$

where,  $D$  is a diagonal matrix in which its primary diagonal elements are the eigenvalues of  $\text{cov}(X)$  and  $P$  is the orthonormal eigenvectors of  $\text{cov}(X)$  arranged in columns-wise. Therefore,  $\text{cov}(Y)$  can then be rewritten as:

$$\text{cov}(Y) = E[A(PDP^T)A^T] \quad (8)$$

By substituting  $A = P^T$  and  $A^T = P$  into Eq. 8 gives:

$$\text{cov}(Y) = E[P^T(PDP^T)P] \quad (9)$$

Since,  $P$  is also an orthonormal matrix,  $P^TP = I$ , it follows that:

$$\text{cov}(Y) = D \quad (10)$$

It is therefore, evident to say that by choosing a matrix  $A$  that consist of the eigenvectors of  $\text{cov}(X)$ , a new orthogonal coordinate system  $Y$  based on the knowledge of the means and correlations of the original data is successfully produced. The eigenvectors that corresponds to the larger eigenvalues are termed as principal components and they are arranged according to the eigenvalues from the highest to the lowest in matrix  $A$ . The first principal components represents the most significant relationships of the original data. By following the theorem that the inverse of an orthonormal matrix is its transpose, the inverse transformation of  $Y = AX$  or  $Y = P^TX$  can then be expressed as:

$$X = ATY \text{ or } X = PY$$

Thus, by applying derived expression of PCA above, the original data are transformed to a new axes defined by the principal component line of best fit. As shown in Fig. 2a, the principal component line of best fit is another option to represent data regression as compared to the line of best fit for which the sum of square distances of points from the line is a minimum. It is seen in Fig. 2b that the original data are re-express in an axes defined by the first principal component such that data decorrelation is achieved as the principal components that accounts for most variation is able to represent that original data.

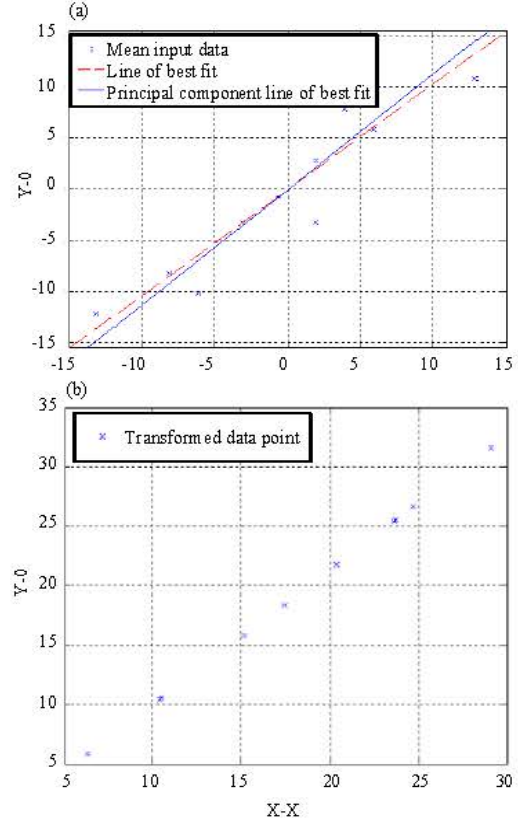


Fig. 2: Outcome of applying principal component analysis for two sets of data points,  $X$ ; a) Plot of the first eigenvectors of matrix  $a$  produces the principal component line of best fit and b) Original input data is transformed into a new axes based only on first eigenvector or the principal component,  $X = PY$

In practice, the mean of the original image is not null. In view of that PCA has to start with the elements of the original image minus the mean of each data dimension (column-wise). The studies by Richardson (2009) and Stolevski (2010) proposed that the mean values are obtained from the row dimension have to be rectified. The computational of eigenvectors of the mean-minus matrix is tedious but it can now be computed by numerical packages such as Octave, Mathematica and LAPACK. In MATLAB environment, `princomp` is the command used to compute the eigenvector of the input matrix. Equation 12 shows that the output of the command is a feature matrix,  $P$  that contains all principal component arranged according to the descending order of the eigenvalues:

$$P = \begin{bmatrix} P_{11} & P_{12} & \cdots & - \\ P_{21} & P_{22} & \cdots & -P \\ \vdots & \vdots & \ddots & \vdots \\ P_{n1} & P_{n2} & \cdots & P(n \times p) \end{bmatrix} \quad (11)$$



The lower the value of p, the higher the Compression Ratio (CR). These relationships can be expressed as:

$$CR = 1 - \frac{np}{mn} \quad (12)$$

There are studies suggested local compression approach by preserving the Regions of Interest (ROIs) on medical images. By retaining the image quality of certain diagnostically important features on the images, the compression level is said to have achieved higher without severely compromising the image quality and affecting the assessment done by the medical professionals.

An overview of the state-of-the-art ROI compression techniques applied to medical images can be found by Doukas and Maglogiannis (2007). Several methods were mentioned in the study including MAXSHIFT, EZW-based ROI, ROI-VQ and general scaling method. A hybrid coder of lossless ROI compression on colon CT images was proposed by Gokturk *et al.* (2001) and ROI segmentation was done using mathematical morphology. By Gokturk *et al.* (2001), a wavelet-based compression scheme was applied to heart MRI image and ROI was segmented by an ellipse fitted by means of genetic algorithm. The first attempt to compress ROI in medical image using PCA was proposed by Taur and Tau (1996). In their research, a simple mean thresholding for blocks of pixels were used to segment the breast tissues. The resulting ROI were either oversegmented or undersegmented and PCA algorithm imposed on block information as proven by Lim *et al.* (2014a, b), produces very poor image quality. PCA was also employed in a region-based color images compression but it was used only determine the spatio-chromatic information of a colour image, so that, the existing spatial correlations between the transform coefficient are removed and encoded using linear prediction (Carevic and Caelli, 1997).

By Radha (2011), the foreground of the medical images was identified as the ROI and different compression algorithm such as PCA, EZW, Set Partition In Hierarchical Tree (SPIHT) and Zero-Tree Entropy (ZTE) coding were used to compress the foreground. However, a crude assumption had been made in the research in which ROI is defined as the foreground of the image but a ROI are in fact the area of interest within the foreground. Results comparison from this research showed that PCA-based models produce higher compression gain with better PSNR and faster processing speed. The results has also provided a base ground behind the selection of PCA algorithm in this research.

It is only recently that region-based image compression using PCA were discussed again (Lim *et al.*, 2014a, b; Manpreet and Wasson, 2015). PCA is inherently restricted to square information and hence an approach

that compress any arbitrary-shape ROI using PCA was proposed. However, one of the limitation of the study is that the selection of ROI was done manually. By Manpreet and Wasson (2015), fractal lossy compression for non-ROI have been implemented but the segmentation technique used was not discussed and it is assumed that the segmentation was done manually. In this study, an automated segmentation of ROI on MRI brain images based on ellipse fitting will be employed and the ROI selected will be preserved and the non-ROI area will be compressed by PCA algorithm. The novelty of this study lies in investigating the compression efficiency of PCA algorithm on a region-based brain images segmented by a robust segmentation technique.

## MATERIALS AND METHODS

As shown in Fig. 3, the ROI in this study is defined as the area of pixels denoted by the abnormalities such as tumor or lesion. The non-ROI are the normal-appearing brain anatomy and the background contains no information depicting the brain anatomy. A model as shown in Fig. 4 is proposed in order to achieve the

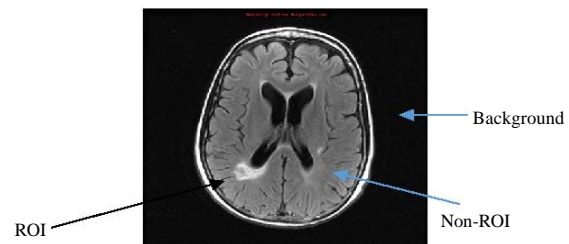


Fig. 3: Definition of ROI

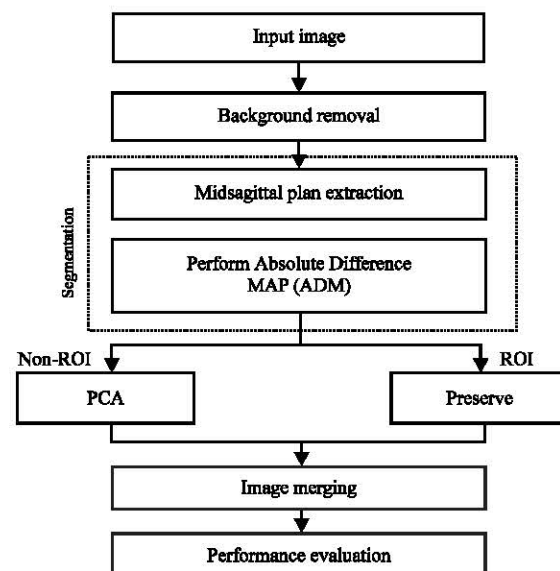


Fig. 4: The general framework for proposed model

objective of this study. In this model an automated segmentation algorithm based on brain symmetry will be employed to only select the ROI cluster pixels. Once the ROI and non-ROI are separated, the non ROI region that accounts for more compression weightage are compressed using PCA algorithm whilst the ROI that is crucial for diagnostic will not be compressed.

**Brain images:** A diverse collection of MRI brain images, illustrating various brain condition are made publicly available in an online platform called Radiopaedia.org. In this study, 10 clear axial brain images from Radiopaedia.org, regardless of the pulse sequences were selected and used under site permission. The images were carefully selected, so that, they consists of only a single ROI. The raw images were stored in JPEG image format files (.jpg) and the image size is at 24 bits per channel, ranging in size from 768×1024 to 1024×1024.

**Background removal processing:** The input image will undergo preprocessing stage to remove noise and to ensure contrast uniformity. One of the major step in preprocessing is to null the background pixels into zero, so that, area beyond the brain anatomy contains no redundant data pixels. Resizing the images in all cases is not considered in this study because the algorithm proposed here is size independent. The resultant compression ratio is always relative to the original image size. The first stage in background removal processing as shown in Fig. 5 is to binarize the input image by using Otsu's gray thresholding. In order to perform Otsu's gray thresholding, the color image will first be converted into gray scale. The resultant binary image will be dilated with disk structuring element and the largest connected component will be labelled with its length of the pixel

connectivity calculated. This method works well for axial brain image as the largest connected component usually encloses the skull. Morphology operation is again employed at this step by filling in the holes on the largest connected component. This provides the mask where its background contains only pixels with zero values. The original color image will be multiplied to the mask image to have its background successfully removed.

**MidSagittal Plane (MSP) extraction:** MSP serves as the landmark to best split the brain into halves left and right hemisphere, respectively. In this study, a robust MSP extraction using ellipse fitting method is employed where the skull of the head is assumed to be in elliptic shape. To find the ellipse an algebraic ellipse fitting method where a set of parameters that minimize some distance measure between the data points and the ellipse will be found (Rosin, 1993). The general second-degree equation of a conic is given as:

$$Q(x, y) = ax^2 + bxy + cy^2 + dx + ey + f = 0 \quad (13)$$

If  $b^2 - 4ac < 0$ , Eq. 14 represents an ellipse. The conic that best fits a set of N points can be approached by minimizing the sum of square of algebraic distances  $Q(x_i, y_i)$  (Fitzgibbon *et al.*, 1999):

$$S(u) = \sum_{i=1}^N Q(x_i, y_i)^2 \quad (14)$$

Now, assume that N coordinates of the geometry landmarks of the skull are  $(x_N, y_N)$ . Let, B be the matrix of the geometry landmark and u be the vector of unknown coefficients:

$$U = \begin{bmatrix} a \\ b \\ c \\ d \\ e \\ f \end{bmatrix}; B = \begin{bmatrix} x_1^2 & x_1 y_1 & y_1^2 & x_1 & y_1 & 1 \\ \vdots & \vdots & \vdots & \vdots & \vdots & \vdots \\ x_N^2 & x_N y_N & y_N^2 & x_N & y_N & 1 \end{bmatrix} \quad (15)$$

$Q(x, y)$  can be rewritten as:

$$Q(x, y) = Bu = 0 \quad (16)$$

In order to avoid the trivial solution of  $u = [000000]^T$  u can be solved in the least square sense if constraint is set on the parameters (Gander *et al.*, 1994). In this research, the constraint is set with  $v^T u = 1$  where

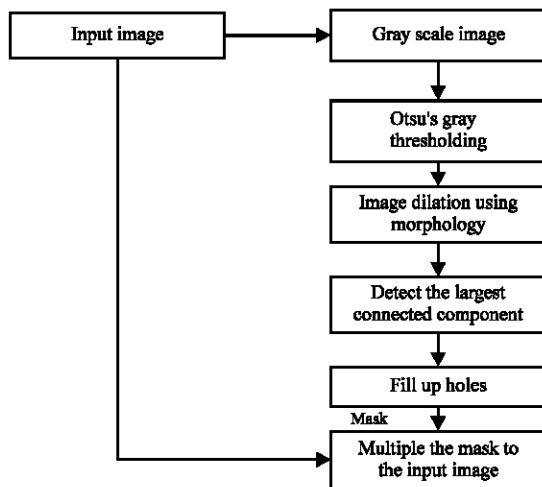


Fig. 5: Flowchart illustrates the steps to null the image background

$v = [100000]^T$ . This constraint forces  $a = 1$  and provides a unique solution. By using constrained optimization, the set up for the problem is structured as minimizing  $S(u) = \|Bu\|^2$  subject to the constraint  $v^T u = 1$  and it can be rewritten as:

$$1 = B^T B u^2 - \lambda (v^T u - 1) \frac{dL}{du} = 2B^T B u - \lambda v^T u = 0 \quad (17)$$

$$v^T u = 1 \quad (18)$$

By algebraically solving Eq. 18 and 19, the unknown coefficient  $u$  is arrived as:

$$u = \frac{(B^T B)^{-1} v}{v^T (B^T B)^{-1} v} \quad (19)$$

With that, the centroid of the ellipse,  $C$  can be found by solving the differential equations shown in Eq. 21:

$$\begin{aligned} \frac{dQ(x,y)}{dx} &= 2ax + by + d = 0 \\ \frac{dQ(x,y)}{dy} &= bx + 2cy + e = 0 \end{aligned} \quad (20)$$

Assuming  $b^2 - 4ac \neq 0$ :

$$C = - \begin{bmatrix} 2a & b \\ b & 2c \end{bmatrix}^{-1} \begin{bmatrix} d \\ e \end{bmatrix} \quad (21)$$

It is also noteworthy that an ellipse is rotated, either left-tilted or right tilted, when the general equation contains the  $xy$  term (Fitzgibbon *et al.*, 1999). In Fig. 6, the  $x$  and  $y$  axes have been rotated about the origin through an acute angle  $\theta$  to produce the  $X$  and  $Y$  axes where:

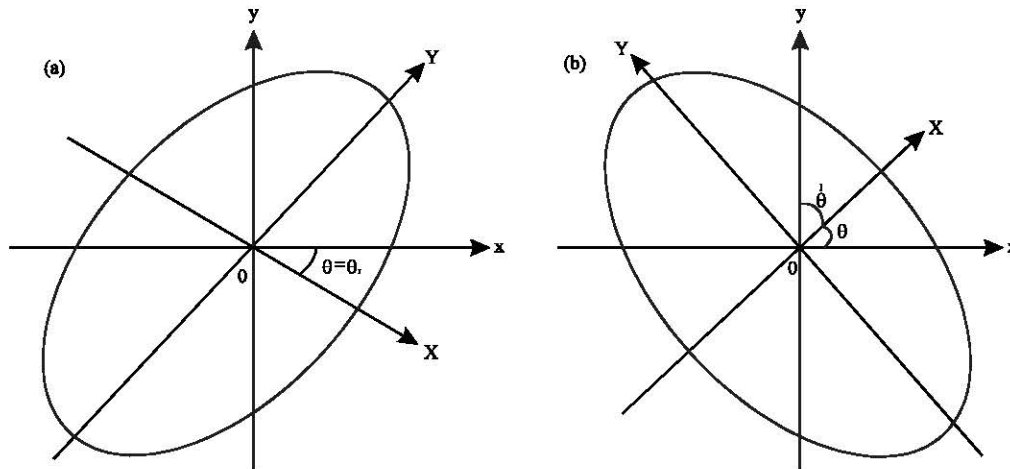


Fig. 6: Brain is assumed as elliptical shape that can be tilted to the; a) Right and b) Left

$$\theta = \frac{1}{2} \tan^{-1} \left( \frac{B}{A-C} \right) \quad (22)$$

The gradient of the semi-minor axis of the ellipse,  $G$  can, hence, be found by employing trigonometry theory:

$$G = \tan \theta = \frac{\sqrt{1 + \cos 2\theta}}{1 - \cos 2\theta} = \sqrt{1 + \left( \frac{A-C}{B} \right)^2} + \frac{A-C}{B} \quad (23)$$

It is noticed that the gradient of the semi-minor axis does not only provide the angle of rotation, it is a metric that indicates whether, the ellipse is right-tilted or left-tilted. The strategy employed in this study is to obtain a perfectly straight image and rotate it manually from  $45^\circ$  to  $+45^\circ$  with a  $5^\circ$  increment. The rotated images will be fed into the MSP algorithm that calculates their corresponding  $G$  values. It is found from the data that for  $G > 1$ , the brain is right-tilted and for  $G \leq 1$ , the brain is left-tilted.

The counter clockwise angle of rotation for right-tilted brain and the clockwise angle of rotation for left-tilted brain is therefore, stated in Eq. 25 and 26, respectively:

$$\theta_r = \tan^{-1} G \quad (24)$$

$$\theta_l = \tan^{-1} \frac{1}{G} \quad (25)$$

After the images are tilted straight, the brain are readily divided into right and left hemisphere according to the realigned MSP.

**Absolute Difference Map (ADM):** Assuming that the pathological hemisphere and normal hemisphere exhibit

brain asymmetrical characteristics, ROI will be detected by performing the ADM between both left and right hemisphere. The hemisphere with ROI will have higher total intensity values as compared to the normal hemisphere. The framework for ADM modified from (Liu *et al.*, 2008) is illustrated in Fig. 7.

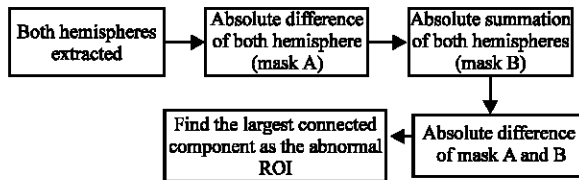


Fig. 7: Flowchart depicts the steps to locate the ROI

## RESULTS AND DISCUSSION

The algorithm were programmed and executed solely in MATLAB platform and it took on an average of 2 sec on an Intel ® Core™ i5 with 2.6 GHz and 6G RAM to compress an image. The automated segmentation algorithm works well on all selected images and it took approximately 1 sec to process an image. In this study, only three out ten images denoted as image 1-3 for each subsequent process were displayed in Fig. 8-11.

On a visual aspect regarding the images tested using the proposed method, all the ROI region has no distortion although, the non-ROI are generally blurred by pixel-blending artifacts and blocking effects as shown in

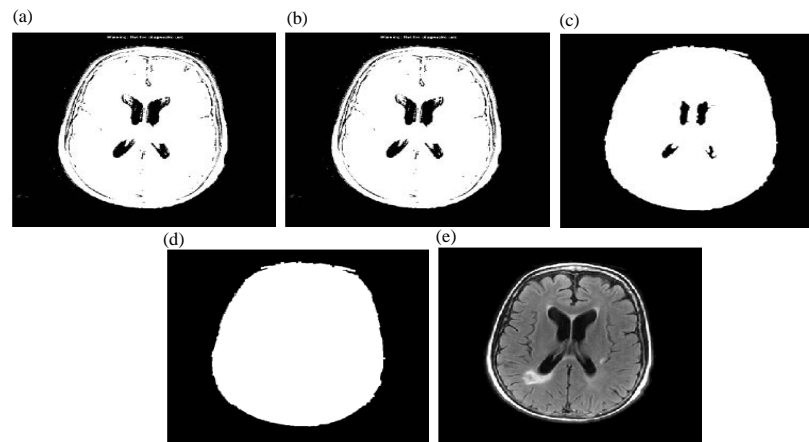


Fig. 8: Sequence of images that go through each step; a) Otsu's thresholding where threshold is set at 0.1; b) Dilation operation; c) Largest connected component detected; d) Hole filing operation and e) Original MRI image with background removed

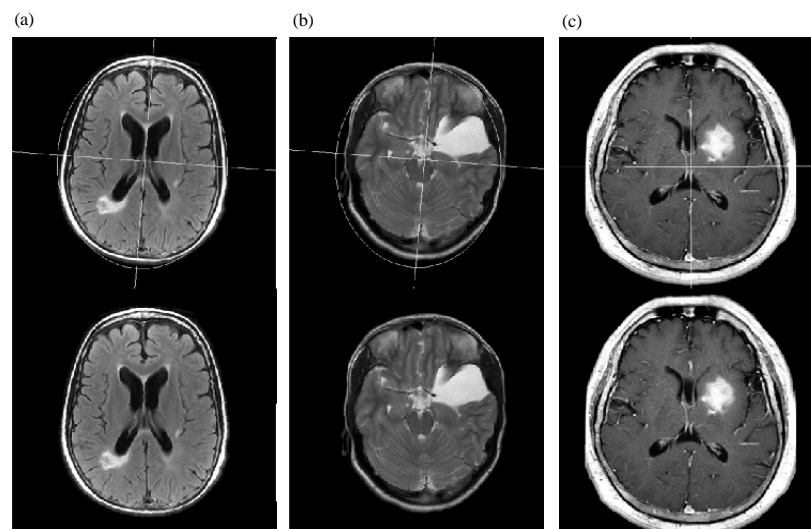


Fig. 9: a) Top: MSP of the brain is located and overlaid on top of the images and b) Bottom tilted brain images are rotated to be in upright position

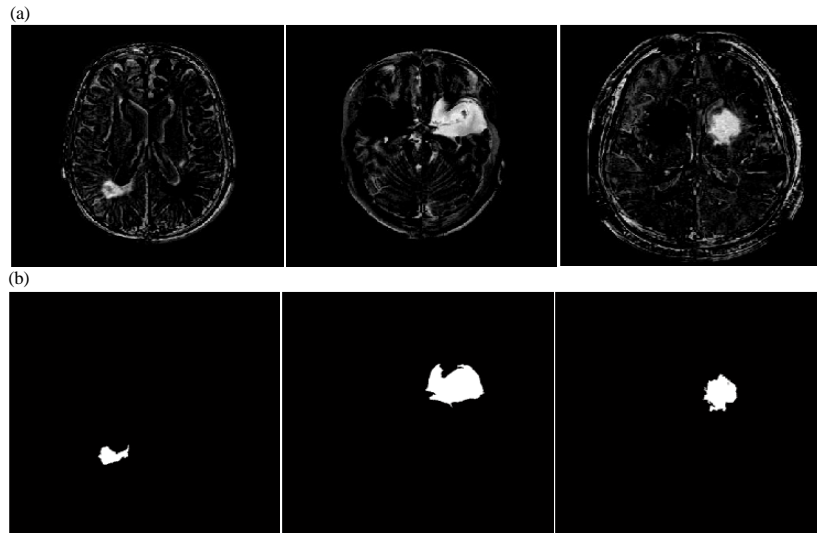


Fig. 10: a) Top: the comparison between left and right hemispheres using ADM algorithm b) Bottom: the segmented ROI for image 1-3, respectively

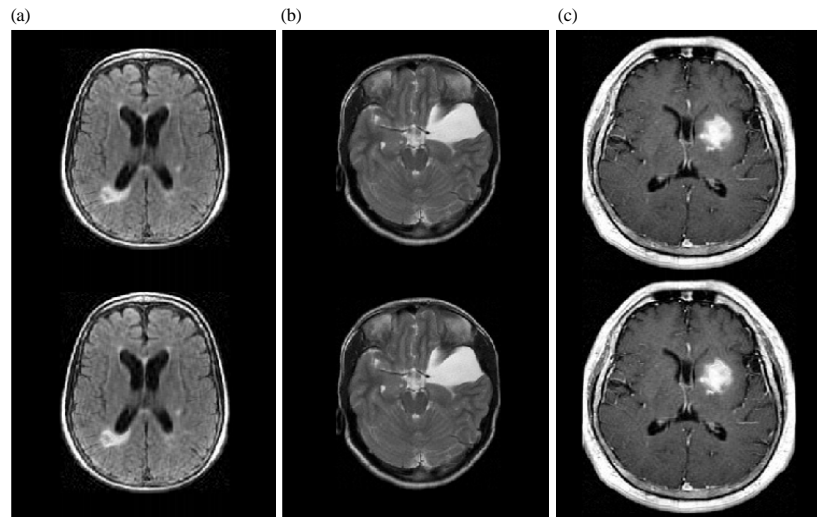


Fig. 11: Output images undergo PCA compression at compression level of 90%; a) Top: without ROI segmentation and b) Bottom: with ROI segmentation

Fig. 11. On the other hand, the images compressed without ROI segmentation are as presumably, distorted regardless of ROI or non-ROI. To measure image distortion level, Peak Signal Noise Ratio (PSNR) as written in Eq. 27 is used. Since, the image under test is a gray image, the dynamic range  $L$  in Eq. 27 is therefore, 255:

$$\text{PSNR} = 10 \log_{10} \frac{L^2}{\text{MSE}} \quad (26)$$

Mean Square Error (MSE) is the amount of distortion or error determined from the difference

between the pixel values in the original image  $X$  and the output image  $Y$ . The formula for MSE can be written as:

$$\text{MSE}(X, Y) = \frac{1}{mn} \sum_{i=1}^m \sum_{j=1}^n (X_{ij} - Y_{ij})^2 \quad (27)$$

The PSNR for images without ROI segmentation and with ROI segmentation were obtained and compared. The chart given in Fig. 12 shows that the PSNR for proposed method on all ten images are higher than those without ROI segmentation ( $p > 0.05$ ) at a compression rate of 90%. The PSNR value increases when the preserved area of ROI is larger.



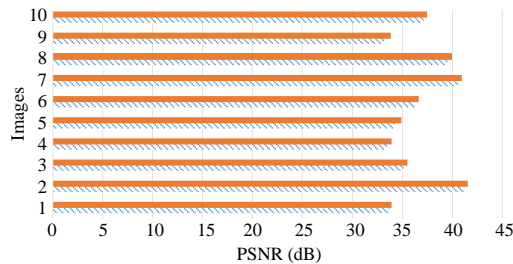


Fig. 12: PSNR for PCA compression with and without ROI segmentation at compression level of 90%

The major constraint of the study is the sensitivity of the MSP algorithm towards uneven or deform skull due to its assumption of brain as elliptical shape. This is not always the case when brain images come into the form of ventral slices that include the ears, nostrils, eyeballs, teeth and neck. However, since, this study serves to investigate the efficiency of the compression algorithm, the ventral slices will not be considered.

## CONCLUSION

In this study, an automated algorithm with the objective of representing the image with the minimum number of bits and with no information loss in ROI has been successfully presented. The front part of the algorithm consists of a specifically designed segmentation technique that employs a robust elliptical approach based on the gradient of the semi-minor axis and the end part of the algorithm is a PCA compression algorithm that serve to partially compress the input image. This is the preliminary attempt to test on the feasibility of coupling an automated segmentation technique with a PCA algorithm. By using PSNR as performance metric at a function of very high compression rate, it was shown that the performance of the proposed region-based algorithm offers improved performance compared to the standard PCA standard. This is promising as it provides an option for region-based compression, permitting better handling of images in a telemedicine network.

## RECOMMENDATIONS

Future work will include comparing the existing method with different compression algorithm implemented by the existing research such as the Embedded Zero-tree Wavelet (EZW) coding, Set Partition In Hierarchical Tree (SPIHT) algorithm, Zero-Tree Entropy (ZTE) coding algorithm and Fractal lossy algorithm. The lossless algorithm such as JPEG-LS or context tree algorithm can be used to compress the ROI region and the lossy

algorithm mentioned above can be used to compress the non-ROI region. Furthermore, the compressed images shall be evaluated by the medical experts to provide a subjective and realistic measure to the performance of the proposed methods.

## REFERENCES

- Carevic, D. and T. Caelli, 1997. Region-based coding of color images using Karhunen-Loeve transform. *Graphical Models Image Processing*, 59: 27-38.
- Dony, R.D., 2001. Karhunen-Loeve Transform. In: *The Transform and Data Compression Handbook*, Rao, K.R. and P.C. Yip (Eds.). CRC Press, Boca Raton, Florida, USA., pp: 1-34.
- Doukas, C. and I. Maglogiannis, 2007. Region of interest coding techniques for medical image compression. *IEEE Eng. Med. Biol. Mag.*, 26: 29-35.
- England, N.H.S., 2016. Diagnostic imaging dataset statistical release. Department of Health, London, England, UK.
- Fitzgibbon, A., M. Pilu and R.B. Fisher, 1999. Direct least square fitting of ellipses. *IEEE. Trans. Pattern Analysis Mach. Intell.*, 21: 476-480.
- Gander, W., G.H. Golub and R. Strebler, 1994. Least-squares fitting of circles and ellipses. *BIT. Numer. Math.*, 34: 558-578.
- Gokturk, S.B., C. Tomasi, B. Girod and C. Beaulieu, 2001. Medical image compression based on region of interest, with application to colon CT images. *Proceedings of the 23rd Annual International Conference of the Engineering in Medicine and Biology Society*, Volume 3, October 25-28, 2001, Istanbul, Turkey, pp: 2453-2456.
- Hotelling, H., 1933. Analysis of a complex of statistical variables into principal components. *J. Educ. Psychol.*, 24: 498-520.
- Lim, S.T., D.F. Yap and N.A. Manap, 2014a. A GUI system for region-based image compression using principal component analysis. *Proceedings of the 2014 International Conference on Computational Science and Technology (ICCST)*, August 27-28, 2014, IEEE, Kota Kinabalu, Malaysia, ISBN:978-1-4799-3241-2, pp: 1-4.
- Lim, S.T., D.F.W. Yap and N.A. Manap, 2014b. Medical image compression using block-based PCA algorithm. *Proceedings of the 2014 International Conference on Computer, Communications and Control Technology (I4CT)*, September 2-4, 2014, IEEE, Langkawi, Malaysia, ISBN:978-1-4799-4555-9, pp: 171-175.

- Liu, S.X., C. Imielinska, A. Laine, W.S. Millar and E.S. Connolly *et al.*, 2008. Asymmetry analysis in rodent cerebral ischemia models. *Acad. Radiol.*, 15: 1181-1197.
- Manpreet, K. and V. Wasson, 2015. ROI based medical image compression for telemedicine application. *Procedia Comput. Sci.*, 70: 579-585.
- Pearson, K., 1901. On lines and planes of closest fit to systems of points in space. *Phil. Mag.*, 2: 559-572.
- Radha, V., 2011. A comparative study on roi-based lossy compression techniques for compressing medical image. *Proceedings of the International Conference on World Congress on Engineering and Computer Science Vol. 1*, October 19-21, 2011, WCECS, San Francisco, California, USA., ISBN:978-988-18210-9-6, pp: 1-6.
- Radiologist, C.A.O., 2011. CAR standards for irreversible compression in digital diagnostic imaging within radiology. *Canada Health Infoway*, Toronto, Ontario.
- Richardson, M., 2009. Principal component analysis. Master Thesis, Faculty of Natural Sciences and Engineering, University of Ljubljana, Ljubljana, Slovenia.
- Rosin, P.L., 1993. A note on the least squares fitting of ellipses. *Pattern Recognit. Lett.*, 14: 799-808.
- Schlens, J., 2014. A tutorial on principal component analysis. Master Thesis, Cornell University, Ithaca, New York, USA.
- Stolevski, S., 2010. Hybrid PCA algorithm for image compression. *Proceedings of the 18th International Conference on Telecommunication Forum TELFOR*, November 23-25, 2010, University of Belgrade, Belgrade, Serbia, pp: 685-687.
- Taur, J.S. and C.W. Tao, 1996. Medical image compression using principal component analysis. *Proceedings of the International Conference on Image Processing Vol. 2*, September 19-19, 1996, IEEE, Lausanne, Switzerland, ISBN:0-7803-3259-8, pp: 903-906.
- Wang, R., 2012. *Introduction to Orthogonal Transforms: With Applications in Data Processing and Analysis*. Cambridge University Press, Cambridge, UK., ISBN:978-0-521-51688-4, Pages: 568.